

**Figure 1.** NO stretching frequencies of nitrosyls of known structure, following Pirug et al., and of adsorbed NO. The numbers 1 and 3 refer to the sequence in which the species appear on the surface as a function of exposure. This figure is taken from Figure 6.12 of ref 9. (Reprinted with permission from ref 9. Copyright 1982, Academic Press.)

Gland and Sexton<sup>11</sup> also studied the vibrational spectra of NO on Pt(111) by EELS, LEED, and Auger. At 100 K and low coverage two frequencies at 350 and 1470  $\text{cm}^{-1}$  were observed, while at high coverage four frequencies at 290, 450, 1490, and 1710  $\text{cm}^{-1}$  were observed. The interpretation was that NO adsorbed initially in a bridge site; then the repulsive interactions due to coverage increasingly forced NO molecules into linearly bonded on-top sites.

Gorte and Gland<sup>12</sup> measured the vibrational spectra of NO on Pt(110) by the same methods as outlined above. At 230 K and low coverage two frequencies at 390 and 1610  $\text{cm}^{-1}$  were observed and assigned to bridge-bonded NO. At high coverage three frequencies, at 220, 1620, and 1760  $\text{cm}^{-1}$ , were observed and assigned to bridge and on-top adsorbed NO.

Infrared spectra of NO adsorbed on Pt(111) and polycrystalline Pt foils were measured by Dunn et al.<sup>13</sup> Relatively intense absorption bands were found over the range 1450–1780  $\text{cm}^{-1}$ , depending on the temperature, coverage, and impurities. A model based on an assumed interaction force constant coupling for NO molecules adsorbed on adjacent sites accounts quantitatively for most of the spectroscopic observations. But the nature of the short-range coupling force is not clear.

For NO adsorption on nickel, there are also two adsorption states observed. Carley et al.<sup>14</sup> investigated NO adsorption on Ni polycrystalline films by XPS. Two molecularly adsorbed NO species were found, a N(1s) peak at about 399 eV was assigned to bent NO, a second one at 402 eV to linearly bonded NO.

Lehwald, Yates, and Ibach measured the vibration spectra of NO on Ni(111) by EELS combined with LEED and Auger.<sup>15</sup> At 150 K and all coverages a frequency varying from 1490 to 1600  $\text{cm}^{-1}$  was observed and assigned to N–O stretching vibration of twofold bridge-adsorbed NO. At low coverage two additional vibrations at 410 and 740  $\text{cm}^{-1}$  were observed and assigned to Ni–N stretching and Ni–N–O bending vibration of a bent configuration. At high coverage the 740- $\text{cm}^{-1}$  loss disappeared and the 410- $\text{cm}^{-1}$  loss shifted to  $\sim 360 \text{ cm}^{-1}$ . This was assigned to

surface–N stretching vibration of a linear or perpendicular configuration.

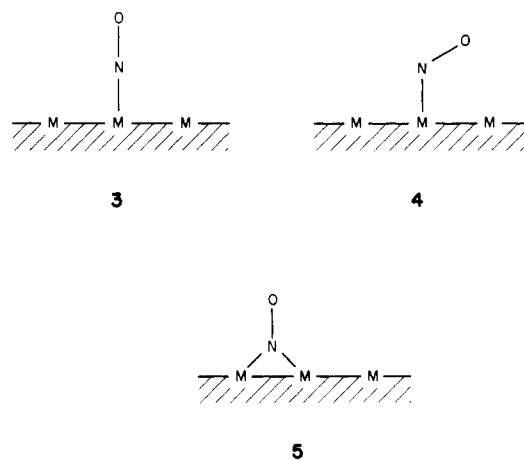
Netzer and Madey studied the adsorption of NO on Ni(111) by ESDIAD (electron stimulated desorption ion angular distributions) and LEED.<sup>16</sup> They found that NO appears to be bonded perpendicular to the Ni(111) surface at all coverages at 80 K. Heating the 80 K layer leads to a striking structural change which they interpret as the formation of bent NO in the range  $120 \leq T \leq 250 \text{ K}$ . Upon adsorption at 150 K, only the bent form of NO is present at low coverages; at high coverages the perpendicular form appears, in agreement with the EELS data of Lehwald, Yates, and Ibach.<sup>15</sup>

Stöhr et al. have studied the orientation of chemisorbed NO on Ni(100) by surface-adsorption fine-structure measurements at 80 K for NO at saturation ( $\sim 1/2$  monolayer) coverage and found the NO molecule to be aligned along the surface normal, within  $10^\circ$ .<sup>17</sup>

Peebles, Hardegree, and White studied the adsorption of NO on Ni(100) at 90 K. They observed two forms of molecular NO and assigned these as bridge-bonded NO at low coverage and linearly bonded NO at high coverage.<sup>18</sup>

NO adsorption on other transition-metal surfaces has also been studied. One example is the extensively studied Ru surface.<sup>19</sup> Two or three molecularly adsorbed states were observed and interpreted within the framework of threefold bridge, twofold bridge, and on-top site models.

The controversy that exists in the literature concerning the interpretation of the vibrational frequencies observed is essentially between *adsorbate geometry* (for instance on-top linear (3) vs. bent (4)) and *adsorption site* (for instance on-top linear (3) vs. bridging linear (5)) models. A further complication is the possible



involvement of N–N bonded  $\text{N}_2\text{O}_2$  dimers on the surface.

The argument for an adsorbate geometry interpretation is mainly based on the two low-frequency vibrations observed. The adsorption site model proponents argue that the assignment of the low-frequency band in the 200–600- $\text{cm}^{-1}$  region is not possible at the present time and that the correct number of frequencies for bent NO has been observed only on few surfaces.

We hoped that theory could contribute something to an understanding of these bonding alternatives. To this end we have carried out extended Hückel tight binding calculations of NO on Ni(111) in various geometries and different adsorption sites. The surface was modeled by a three-layer Ni slab, and the NO was adsorbed on one face of that slab. The effect of coverage was studied in some detail. The computational assumptions and pa-

(11) Gland, J. L.; Sexton, B. A. *Surf. Sci.* **1980**, *94*, 355.

(12) Gorte, R. J.; Gland, J. L. *Surf. Sci.* **1981**, *102*, 348.

(13) Dunn, D. S.; Severson, M. W.; Hylden, J. L.; Overend, J. *J. Catal.* **1982**, *78*, 225. Dunn, D. S.; Severson, M. W.; Golden, W. G.; Overend, J. *J. Catal.* **1980**, *65*, 271. Severson, M. W.; Overend, J. *J. Chem. Phys.* **1982**, *76*, 1584.

(14) Carley, A. F.; Rassias, S.; Roberts, M. W.; Wang, T.-H. *Surf. Sci.* **1979**, *84*, L227.

(15) Lehwald, S.; Yates, J. T., Jr.; Ibach, M. *Proceedings of the Fourth International Conference on Solid Surfaces*; Institute of Physics and Physical Society: London, 1980; Vol. 1, p 221.

(16) Netzer, F. P.; Madey, T. E. *Surf. Sci.* **1981**, *110*, 251.

(17) Stöhr, J.; Baberschke, K.; Jaeger, R.; Treichler, R.; Brennan, S. *Phys. Rev. Lett.* **1981**, *47*, 381.

(18) Peebles, D. E.; Hardegree, E. L.; White, J. M. *Surf. Sci.* **1984**, *148*, 635.

(19) Umbach, E.; Kulkarni, S.; Feulner, P.; Menzel, D. *Surf. Sci.* **1978**, *88*, 65. Thiel, P. A.; Weinberg, W. H.; Yates, J. T., Jr. *J. Chem. Phys.* **1979**, *71*, 1643. Conrad, N.; Scala, R.; Stenzel, W.; Unwin, R. *Surf. Sci.* **1984**, *145*, 1.

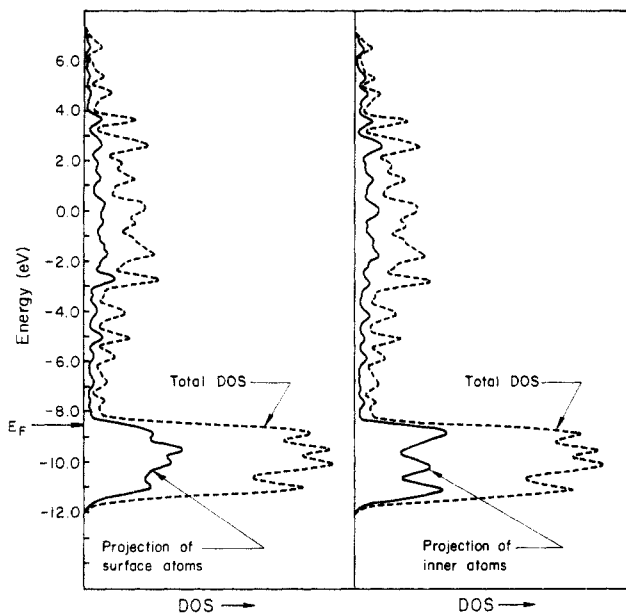


**Figure 2.** Projected DOS of surface and inner layers of the Ni(111) three layer slab. In better, self-consistent calculations similar dispersion effects are observed, but the surface states are more skewed toward the Fermi level.

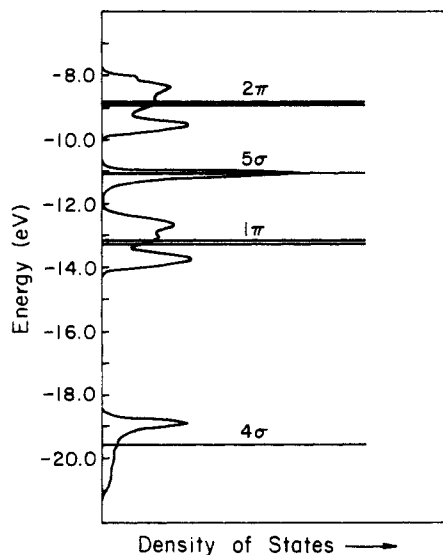
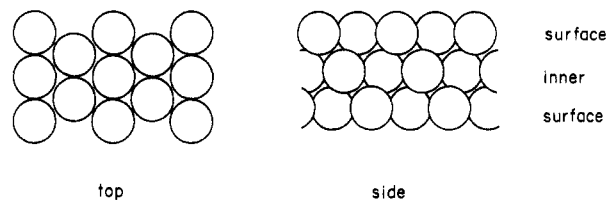


**Figure 3.** The density of states of monolayer NO corresponding to full coverage on Ni(111). The straight lines or sticks are the molecular orbitals of isolated molecular NO.

rameters are listed in the Appendix. Throughout our work we were aided by decompositions of the density of states (DOS) and the unique interpretational tool of crystal orbital overlap population (COOP) curves.<sup>20</sup>

### The Ni(111) Surface

Consider the three-layer slab model of the Ni(111) surface, shown in two views in 6. The Ni–Ni distance is taken as 2.40 Å. There are two surface layers in this slab, and one inner layer, approximating the bulk. The total DOS and the contributions of a surface and inner layer to the total DOS are shown in Figure 2. As expected, the inner layer DOS has a greater dispersion than the outer or surface layers. This leads to a negative charging of the surface, an effect noted and analyzed by other workers<sup>21</sup>

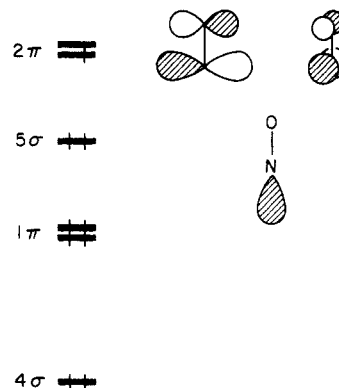


6

as well as by us.<sup>22</sup> The 4s band penetrates substantially the metal 3d band, so that for the surface layer the calculated configuration is  $d^{9.277}s^{0.628}p^{0.200}$ .

### NO Isolated and Various Monolayers Assembled from It

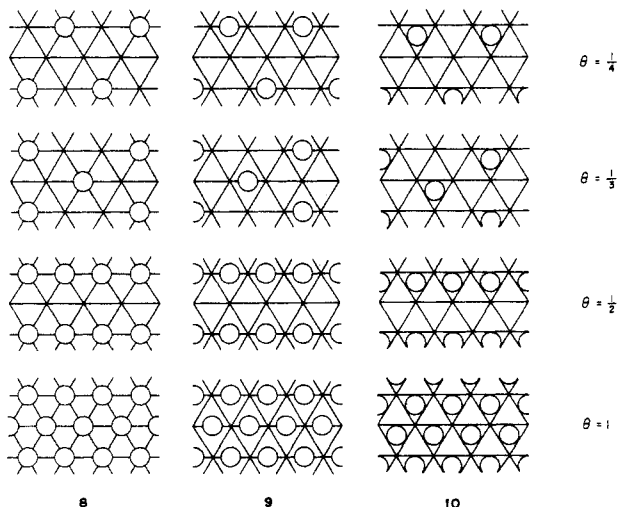
The orbitals of nitric oxide are well-known and are shown schematically in 7. They resemble those of CO, except that they



7

are lower in energy, especially the NO  $\pi^*$ . This is what makes the nitrosyl group such a good electron acceptor. An odd electron occupies the  $2\pi$  or  $\pi^*$  level. The NO overlap population computed is 1.231 at the assumed 1.1-Å internuclear separation.

The spectra of NO adsorbed on Ni, Pt, and Ru surfaces are coverage dependent. We thus must consider varying degrees of coverage. Four arbitrary but well-defined coverages are shown for Ni(111) with NO in an *on-top* site 8, in a *twofold bridging* site, 9, and in a *threefold bridging* or hollow site, 10. The



distances of approach between NO molecules are 4.98, 4.32, and 2.49 Å for coverage,  $1/4$ ,  $1/3$ , and 1, respectively, and 4.32 and 2.49 Å for the particular example of coverage  $1/2$  displayed.

(20) Hughbanks, T.; Hoffmann, R. *J. Am. Chem. Soc.* **1983**, *105*, 1150.  
 (21) Shustorovich, E.; Baetzold, R. C. *J. Am. Chem. Soc.* **1980**, *102*, 5989.  
 Shustorovich, E. *J. Phys. Chem.* **1982**, *86*, 3114. Shustorovich, E. *Solid State Commun.* **1982**, *44*, 567. Feibelman, P. J.; Hamann, D. R. *Solid State Commun.* **1979**, *31*, 413. Desjonqueres, M. C.; Spanjaard, D.; Lassailly, Y.; Guillot, C. *Solid State Commun.* **1980**, *34*, 807.

(22) Saillard, J.-Y.; Hoffmann, R. *J. Am. Chem. Soc.* **1984**, *106*, 2006.

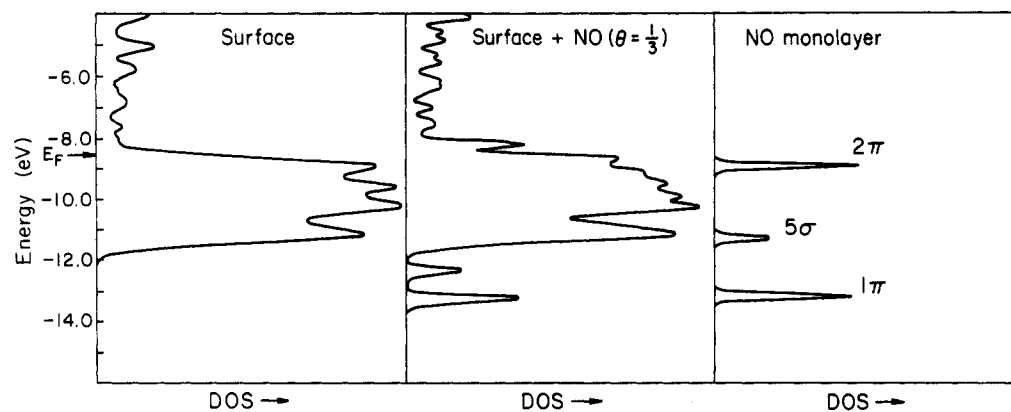


Figure 4. The density of states of a Ni(111) surface layer, a Ni(111) surface layer + on-top adsorbed NO with coverage,  $1/3$ , and monolayer NO.

TABLE I: Different Adsorption Sites

	on-top	twofold bridge	threefold bridge	free NO
overlap populations				
Ni-N	0.822	0.583	0.483	0
N-O	1.034	0.968	0.923	1.231
NO electron densities				
$4\sigma$	1.844	1.801	1.785	2.0
$1\pi_x$	1.984	1.903	1.899	2.0
$1\pi_y$	1.984	1.957	1.957	2.0
$5\sigma$	1.724	1.737	1.758	2.0
$2\pi_x$	0.908	1.265	1.171	0.5
$2\pi_y$	0.908	0.891	1.171	0.5
surface metal electron density change				
$\Delta s$	-0.062	-0.051	-0.118	0
$\Delta p_z$	0.171	0.078	0.033	0
$\Delta d_{z^2}$	-0.616	-0.189	-0.042	0
$\Delta d_{x^2-y^2}$	0.055	-0.034	-0.124	0
$\Delta d_{xy}$	0.055	-0.099	-0.124	0
$\Delta d_{xz}$	-0.572	-0.376	-0.197	0
$\Delta d_{yz}$	-0.572	-0.134	-0.197	0
$\Delta E$ , eV	-3.067	-4.130	-4.240	

Calculations were carried out on each of these two-dimensional NO adlayers (no metal surface as yet). In the layers with coverage  $1/4$  or  $1/3$  the NO...NO separations are too large for any effective interactions, so no significant band widths develop. This is not so at full coverage, where the resultant DOS is shown in Figure 3. Note the larger widths of the  $\pi$  bands—the initial overlap between molecules is through their  $\pi$ -type contacts. The effects of molecule-molecule interaction even at this high coverage are small; the changes in charges and overlap populations are minor except for a significant equalization of the N and O atomic charges. The  $\theta = 1/2$  coverage mode is predictably intermediate and locally anisotropic at each NO.

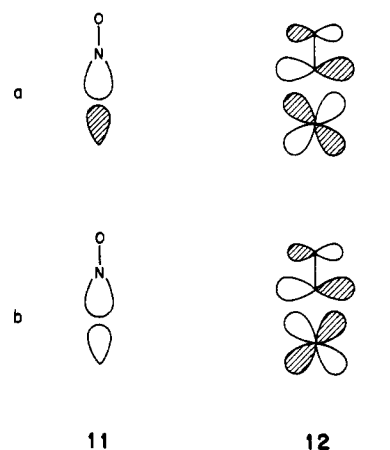
#### A Typical NO-Metal Surface Interaction

We now have a metal surface, modeled by a three-layer slab of Ni(111), and an adsorbing monolayer of nitric oxides. Let us choose as typical intermediate coverage of  $1/3$ , an on-top geometry (see 8) with Ni-N 1.68 Å, and see how the bonding takes place.

There is strong bonding of NO to the surface. Column 1 of Table I indicates phenomenologically what takes place, as does Figure 4, the DOS of the component surface and adlayer isolated and assembled. One sees substantial depletion of NO  $5\sigma$  and a very large increase in the population of the  $\pi^*$  orbital,  $2\pi$ . In free neutral NO there is one electron in the  $2\pi$ , while in the surface + NO one calculates 1.82 electrons, in an orbital that has room for four electrons. This population of NO  $2\pi$  is largely responsible for the decrease in N-O overlap population. The electron density transferred to  $2\pi$  comes largely from surface  $\pi$  orbitals,  $xz$  and  $yz$ . It also comes, in an indirect but important way, from surface  $z^2$  orbitals. What happens is something very similar to the case

of CO adsorption, as analyzed by us<sup>23</sup> and by others.<sup>24,27</sup> The argument goes as follows:

It is no surprise that the primary interactions of CO and NO with surfaces are similar to those in discrete complexes of these ligands with mononuclear or polynuclear transition-metal complexes. In particular there is forward donation from diatomic  $5\sigma$ , and back donation into diatomic  $2\pi$ . The relevant local bonding and antibonding combinations are shown in 11 and 12. Orbitals



like these are easily found in discrete complexes and, while translationally delocalized, can also be identified in the surface-adsorbate systems. But there is one important difference between the discrete complex and the surface. In the discrete or molecular complex the antibonding combination 11a is empty and the bonding one 11b is filled. Similarly for 12a and 12b. Since the metal-based hybrid, mainly  $z^2$ , is initially unoccupied, and the metal  $xz, yz$  initially full, the sense of electron drift is clear: population of  $z^2$ , depopulation of  $xz, yz$  as a result of bonding.

It is different for the surface. The metallic delocalization results in near filling of both  $z^2$  and  $xz, yz$  bands (the computed configuration is  $d^{9.277}s^{0.628}p^{0.200}$  for our Ni(111) surface layer). The same interactions occur, but now the  $\sigma$  bonding between  $5\sigma$  of NO and surface  $z^2$  orbitals pushes some of the initially nearly fully populated  $z^2$  surface levels above the Fermi level. There is loss of electron density from both  $z^2$  and  $xz, yz$ .

We analyzed this situation in detail for CO. For NO we only repeat the salient feature of the analysis—an “interaction diagram” in Figure 5 for separate adsorbate and surface  $5\sigma$  and  $z^2$  levels, and a decomposition of the composite surface and adsorbate levels into  $5\sigma$  and  $z^2$  contributions of the fragments. The same figure shows a similar interaction diagram for  $2\pi$  and  $xz, yz$ . It is these

(23) Sung, S.-S.; Hoffmann, R., to be submitted for publication.

(24) Blyholder, G. *J. Phys. Chem.* **1964**, *68*, 2772. Anderson, A. B.; Hoffmann, R. *J. Chem. Phys.* **1974**, *61*, 4545. Anderson, A. B. *J. Chem. Phys.* **1976**, *64*, 4046. Kobayashi, H.; Yoshida, S.; Yamaguchi, M. *Surf. Sci.* **1981**, *107*, 321. Kobayashi, H.; Yamaguchi, M.; Yoshida, S.; Yonezawa, T. *J. Mol. Catal.* **1983**, *22*, 205. van Santen, R. A. *Proceedings, 8th International Congress on Catalysis 1984, Berlin*; Verlag Chemie International: Weinheim.

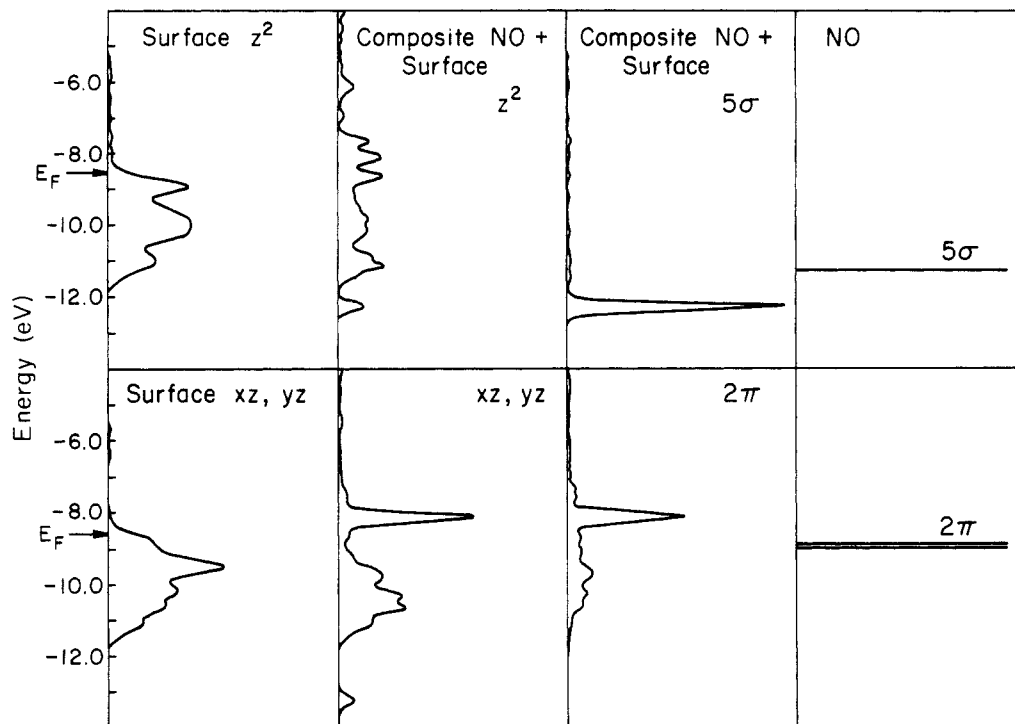


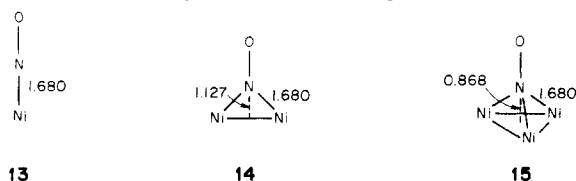
**Figure 5.** Projected DOS of NO and Ni surface layer orbitals separated (a,d) and in the on-top adsorption system (b,c).

kinds of diagrams which are the basis for the qualitative arguments layed out above, and they show crystal-clear the  $\sigma$  and  $\pi$  interactions that matter. The only important way in which NO differs from CO is the expected one: the  $2\pi$  of free NO is lower in energy than that of free CO; NO is a better  $\pi$  acceptor. Using Bremsstrahlung spectroscopy, Rogozik, Küppers, and Dose found that the NO  $2\pi$  derived level on Pd(100) is 3 eV closer to Fermi level than that of CO and extends down to the Fermi level.<sup>25</sup>

Still another way in which we have found it useful to follow bonding changes is through the aforementioned crystal orbital overlap population or COOP curves. These are overlap population weighted densities of states, the differential version of the overlap population between two atoms. As a function of energy the states in the crystal are analyzed with respect to their bonding or antibonding character: a positive COOP value means the states at the energy are on the average bonding, a negative value means that they are antibonding between the specified pair of atoms. Such a curve is shown for the on-top adsorption in Figure 6. The solid line is Ni-N, the dashed line N-O. Note the NO bonding picked up as one sweeps through the  $1\pi$  peak, and the Ni-N bonding as one moves through  $5\sigma$  (11a). In the d band (-7 to -11 eV) region there is clear evidence of Ni-N bonding (from metal- $2\pi$  interactions, 12b) near the bottom of the band, and Ni-N antibonding (from metal- $2\pi$ , 12a, and metal- $5\sigma$ , 11a, interactions) near the top of the band. The NO bonding is interpreted by the same interactions.

#### Different Adsorption Sites, NO Perpendicular to Surface

The previous section looked at a typical bonding pattern, that of linear, on-top NO. Now we will examine in somewhat less detail other adsorption sites. We will keep the NO bond perpendicular to the surface, a fixed Ni-N distance of 1.680 Å, and a coverage of  $1/3$ . The sites in question are on-top 13, a twofold bridge 14, and a threefold bridge, 15. The assumption of a fixed Ni-N



13

14

15

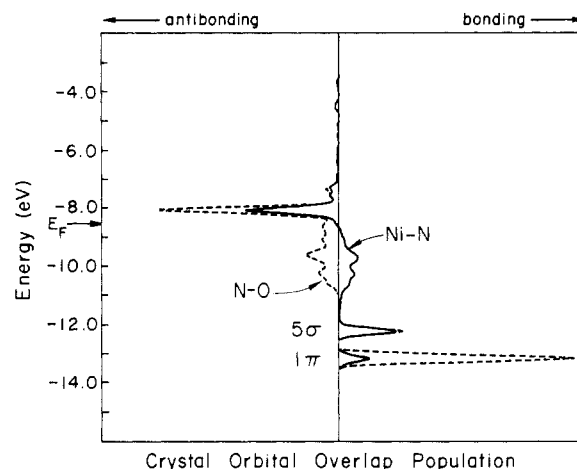
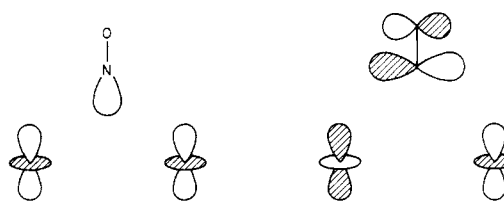


**Figure 6.** Crystal orbital overlap population of the NO-Ni(111) adsorption system: in an on-top site.

distance, which of course leads to a variable N-surface perpendicular contact, is the most worrisome. But in the absence of a reliable method of calculating equilibrium geometries of surface-adsorbate systems, and the total energy of the extended Hückel method cannot be trusted for that purpose, this is about the best that we can do.

Let us examine the main interactions in the two bridging cases, and then compare all three adsorption sites. The relevant electron density changes are in Table I.

The interaction in the twofold bridge site is somewhat more complicated than for NO on-top. The  $z^2$  orbital interacts with both  $\sigma$  and  $\pi$  orbitals of NO, as shown in 16 and 17. Similarly,



16

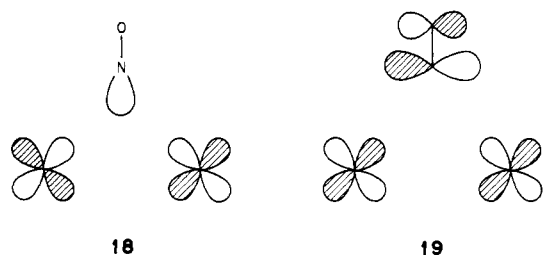
17

TABLE II

coverage bending angle	on-top			twofold bridge			threefold bridge		
	1 0°	1/3 0°	1/3 60°	1 0°	1/3 0°	1/3 60° <sup>a</sup>	1 0°	1/3 0°	1/3 60° <sup>b</sup>
overlap population									
Ni-N	0.743	0.822	0.660	0.564	0.583	0.502	0.464	0.483	0.100 <sup>c</sup>
N-O	0.937	1.034	0.852	1.012	0.068	0.958	0.901	0.923	1.008
$\Delta E$ , eV	-2.484	-3.067	-2.573	-2.756	-4.130	-2.915	-3.695	-4.249	-3.588

<sup>a</sup>Toward hollow site. <sup>b</sup>Toward a neighboring Ni atom. <sup>c</sup>See Table I.

$xz, yz$  interact with both  $\sigma$  and  $\pi$  orbitals of NO, as indicated schematically in 18 and 19. The local symmetry dictates that



the  $2\pi$  orbital interacts with those crystal orbitals which are antibonding between the two Ni atoms, as shown in 19, that is, with the upper part of the d band. The  $2\pi$  orbital energy ( $\sim -9$  eV) is just at the energy of the upper part of d band. This is one reason for the better interaction. Another reason is that the sum of the overlap of  $2\pi_x$  with both  $xz$  ( $2 \times 0.0802$ ) is larger than the  $2\pi_x-xz$  (0.0954) overlap in the on-top site. Similarly, the  $5\sigma$  orbital interacts with the lower part of the d band, which is below the Fermi level, and mixes less with the upper part of d band, which is above the Fermi level. As a result, the  $5\sigma$  contributes less to the unoccupied states, i.e., the  $5\sigma$  electron density changes less upon bridge adsorption.

These changes are reflected in the COOP curve (not shown here) and in the net changes in various indicators listed in Table I. The entries are for one Ni atom (except  $\Delta E$ ). To get an estimate of the overall effect to compare to on-top adsorption one should multiply these indicators by two. It will then be seen that the population of  $2\pi$  is greater in the twofold bridging site, and that this weakens the N-O bond more, and that total Ni-N bonding is greater ( $2 \times 0.583$  compared to 0.822).

The threefold site adsorption<sup>26</sup> leads to still more complicated interactions. We calculate substantially greater Ni-N bond strength (now there are three bonds with overlap populations 0.483 each), a little more N-O bond weakening. The net energy of interaction is comparable to that in the twofold site.

Because of the uncertainty in surface-NO distance and our unwillingness to trust the total energy given to us by the extended Hückel method we are hesitant to make definitive judgments as to the preferred adsorption site, except to say that we think the calculations would seem to favor twofold or threefold bridging to on-top coordination. We base this conclusion (which is at variance with that of Ray and Anderson, who *can* calculate more reliably total energies, and who find the onefold site preferred on cluster models for Pt(111)-CO<sup>27</sup>) as much on the greater smoothness of the electron transfers from various metal orbitals as on the calculated total interaction energy.

### The Effect of Coverage

It is clear from the experimental results that the extent of coverage of the metal surface has an effect on the observed stretching frequencies and the preferred adsorption site. Let us see what the calculations indicate. We examined coverages of

$1/4, 1/3, 1/2$ , and 1 for each of the three adsorption sites, NO perpendicular to the surface in each. The essential results are shown in Table II for the extremes of coverage  $1/3$  and 1.

Note that the N-O overlap population decreases on increasing coverage in the on-top geometry, but the opposite is calculated for twofold bridge adsorption. We can trace the origin of this effect as follows. The general effect of increasing coverage is to increase the dispersion of the adlayer  $2\pi$  (and  $1\pi$ ) bands. In the case of on-top adsorption  $2\pi$  interacts with the entire range of the metal  $xz$  band, and the added dispersion of  $2\pi$  increases that interaction. For twofold bridging adsorption the interaction of  $2\pi$  is selectively with the top of the  $xz$  (and  $z^2$ ) bands, and it appears that the added dispersion has the effect of lowering this interaction.

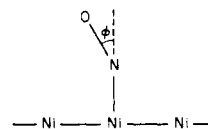
The explanation, however, is not quite that simple. First of all, examination of the details of the orbital charge drifts shows that the decreased population of  $2\pi$  in the bridged site (on increasing coverage) operates primarily through  $2\pi_x$ , the component less involved in bonding. Second, we see signs of NO-NO interactions through bonds, i.e., through the metal surface, not only through space. In this context it should be mentioned that Dunn et al.<sup>13</sup> pointed out that the assumed interaction force constant coupling, rather than the M-N-O angle or different adsorption sites, could be the reason for the observed frequency shift.

In Table II we show also the calculated energy differences per unit cell between the composite and isolated NO + clean surface. The general effect is a smaller bonding energy with increasing coverage, a clear indication of the repulsive NO-NO interactions on the surface. The destabilization with increasing coverage is less for the on-top site, indicating that the tendency to occupy this site will increase at higher coverage.

We note here the earlier theoretical study of Ray and Anderson<sup>28</sup> of the effect of CO coverage on platinum electrode models. Our trends are similar to those observed by these workers.

### Bending Ni-N-O in the On-Top Site

Let us see what happens if we tilt NO from its perpendicular orientation. Consider just the on-top site, coverage =  $1/3$ . Suppose the bending is in the  $xz$  plane, the geometry as shown in 20. The



20

reader is referred to a previous discussion of bending in discrete molecular nitrosyls by one of us,<sup>29</sup> for it makes much of the following discussion, perforce complex, just a little more comprehensible.

The calculational results are shown in Table III as a function of the bending or tilting angle  $\phi$ . For comparison we listed the results for bending in  $yz$  plane, shown as  $60^\circ \perp$ . As  $\phi$  increases from 0 up to  $60^\circ$ , the N-O overlap population decreases. That

(26) The results for the threefold bridge site in Table I are for NO adsorbed in the sites above second layer Ni atoms. There is another alternative threefold bridge site, above third layer Ni atoms. The computational results were examined for both alternatives, and they are very close to each other.

(27) Ray, N. K.; Anderson, A. B. *Surf. Sci.* **1982**, *119*, 35, **1983**, *125*, 803.

(28) Ray, N. K.; Anderson, A. B. *J. Phys. Chem.* **1982**, *86*, 4851. Also see Anderson, A. B. *Surf. Sci.* **1977**, *61*, 119.

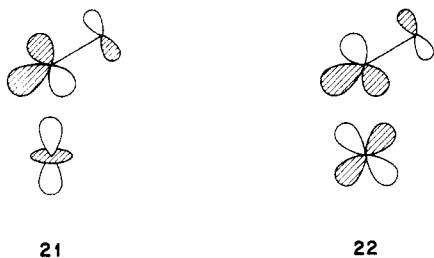
(29) Hoffmann, R.; Chen, M. M. L.; Elian, M.; Rossi, A. R.; Mingos, D. M. P. *Inorg. Chem.* **1974**, *13*, 2666.

TABLE III: Bending in the On-Top Site

	$\phi = 0^\circ$	$\phi = 30^\circ$	$\phi = 60^\circ$	$\phi = 60^\circ \perp$	$\phi = 90^\circ$
overlap population					
Ni-N	0.822	0.792	0.660	0.656	0.491
N-O	1.034	0.998	0.852	0.851	0.983
NO electron densities					
$4\sigma$	1.844	1.852	1.877	1.877	1.901
$1\pi_y$	1.984	1.983	1.981	1.953	1.977
$1\pi_x$		1.976	1.953	1.981	1.906
$5\sigma$	1.724	1.741	1.829	1.833	1.838
$2\pi_y$		0.911	0.929	1.526	0.977
$2\pi_x$	0.908	1.022	1.519	0.925	1.151
surface metal electron density change					
$\Delta s$	-0.062	-0.064	-0.069	-0.070	-0.134
$\Delta p_z$	0.171	0.164	0.139	-0.139	0.098
$\Delta d_{z^2}$	-0.616	-0.608	-0.643	-0.648	-0.603
$\Delta d_{x^2-y^2}$	0.055	0.054	0.048	0.015	0.017
$\Delta d_{xy}$	0.055	0.051	0.014	0.038	0.034
$\Delta d_{yz}$	-0.572	-0.574	-0.580	-0.078	-0.505
$\Delta d_{xz}$	-0.572	-0.532	-0.102	-0.576	-0.229
$E, eV$	-3.067	-2.924	-2.573	-2.549	-1.988

means the NO bond is weakened and the N-O stretching frequency should decrease. This tendency is the same as that invoked in the "linear" and "bent" model interpretations of NO adsorption on the Ni(111) surface, although that model supposes bridge site adsorption, which we will discuss later. As  $\phi$  increases, the Ni-N overlap population decreases also, which should imply that Ni-N vibration frequency should change in the same direction as the N-O stretching frequency. This seems to be in disagreement with experimental observations.<sup>15</sup>

The orbital orientations of  $5\sigma$  and  $2\pi$  of NO,  $z^2$  and  $xz$  of the nearest metal atom are shown in **21** and **22**. In the "linear" case



the  $\sigma$  orbitals of NO are directly pointed toward the metal  $z^2$  (also  $s$  and  $z$ ) orbital, as in **11**. In the "bent" case the  $\sigma$  orbitals start to interact with the  $xz$  orbitals of the metal, **22**, but that interaction is not strong enough to compensate for the loss in the bonding from the  $\sigma$ - $z^2$  interaction. We can see this in the extended surface as well, and it is one reason for the decrease in Ni-N bonding with bending that we calculate. The metal-NO  $\sigma$  antibonding orbitals do not rise above the Fermi level (see discussion around **11**) and consequently more of them are filled.

In the bent geometry the  $\pi$  orbitals are no longer degenerate. As NO bends in the  $xz$  plane, the interaction of  $\pi_y$  orbitals with the metal orbitals, mainly the  $yz$  of the Ni, have changed little. Their electron density changes are very close to the linear case, as Table III shows. However, the  $\pi_x$  orbitals behave quite differently in the linear and bent cases. As indicated in **21** and **22**, the lobes at the N atom "rotate" with the bending NO ligand;  $\pi_x$  and  $\sigma$  orbitals mix and hybridize. The  $xz$  electron density change decreases as NO bends, but that of  $2\pi_x$  increases dramatically. The  $2\pi_x$  interacts with more orbitals, such as  $z^2$ ,  $s$ ,  $z$  of the nearest Ni atom, but its electron density increase comes also from other metal atoms.

A comparison of the projected DOS of  $2\pi_x$  and  $2\pi_y$  in the bent geometry (Figure 7) is helpful for understanding the  $2\pi_x$  electron density increase. Figure 7b is the projected DOS of  $2\pi_y$ . The peak just below -8 eV contains the major part of the  $2\pi_y$  states and is mostly above the Fermi level. In Figure 7a, the projected

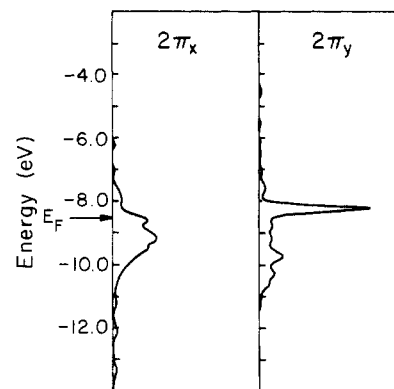


Figure 7. Projected DOS of  $2\pi_x$  and  $2\pi_y$  of NO in the on-top site of Ni(111) with bending angle  $60^\circ$ .

TABLE IV: Bending at the Twofold Bridge Site

	$\phi = 0^\circ$	$\phi = 45^\circ$	$\phi = 90^\circ$
overlap population			
Ni-N	0.583	{ 0.347	{ -0.098
N-O	0.968	{ 0.600	{ 0.479
NO electron densities			
$4\sigma$	1.801	1.819	1.718
$1\pi_{x,z}$	1.903	1.873	1.902
$1\pi_y$	1.957	1.950	1.859
$5\sigma$	1.737	1.759	1.613
$2\pi_{x,z}$	1.265	0.968	1.322
$2\pi_y$	0.891	0.906	1.007
$\Delta E, eV$	-4.130	-2.832	-2.662

DOS of  $2\pi_x$ , the peak disappears and the states are evenly mixed in the metal d block energy region. Therefore  $2\pi_x$  gains more in electron density. This is a major reason for the weakening of the N-O bonding in the bent geometry.

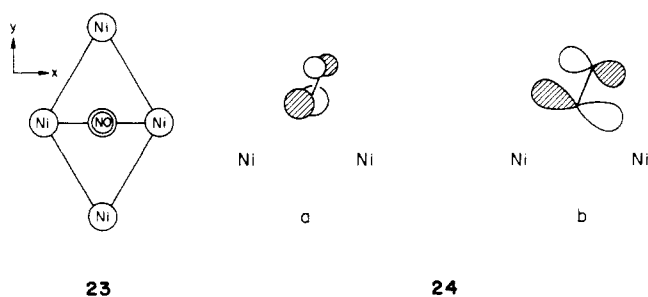
As we can see from Table III, at an extreme bending angle  $90^\circ$  the overlap population between N and O atoms is larger than that at  $60^\circ$ . This kind of bending does not seem to lead a possible NO dissociation pathway.

When NO bends in  $yz$  plane toward the threefold hollow site, the calculational result is very similar to that for bending in  $xz$  plane. At a bending angle of  $60^\circ$ , the overlap populations differ only by 1% one from the other. This is no surprise. We have a local sixfold barrier, and these are hardly likely to produce much differentiation.

As NO bends in the on-top position,  $\Delta E$  monotonically increases and the Ni-N bond strength decreases. The on-top bending configuration does not seem to be a likely candidate for a species explaining the observed low coverage vibrational frequencies.

### Bending While Bridging

We have discussed the bending or tilting of NO when it is in an on-top site—now let us look at the bending in a twofold bridge site. At such a twofold bridge site, **23**, the nearest surface atoms



are along the  $x$  direction, while along  $y$  the distance between NO and surface atoms is larger. At first we consider bending in the  $x$  direction. The calculational results are shown in Table IV.

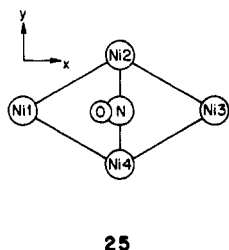
TABLE V: Bending at the Twofold Bridge Site

	$\phi = 0^\circ$	$\phi = 30^\circ$	$\phi = 60^\circ$	$\phi = 90^\circ$
overlap population				
Ni-N	0.583	0.575	0.502	0.387
N-O	0.968	0.966	0.958	1.001
NO electron densities				
$4\sigma$	1.801	1.809	1.818	1.746
$1\pi_y$	1.903	1.899	1.885	1.826
$1\pi_{x,z}$	1.957	1.949	1.928	1.919
$5\sigma$	1.737	1.746	1.771	1.756
$2\pi_y$	1.265	1.272	1.280	0.979
$2\pi_{x,y}$	0.891	0.890	0.976	1.176
surface atom electron density changes				
$\Delta s$	-0.051	-0.055	-0.083	-0.117
$\Delta p_z$	0.078	0.077	0.071	0.062
$\Delta d_{z^2}$	-0.189	0.223	0.215	-0.169
$\Delta d_{x^2-y^2}$	-0.034	-0.050	-0.106	-0.070
$\Delta d_{xy}$	-0.099	-0.087	-0.044	-0.012
$\Delta d_{xz}$	-0.134	-0.123	-0.048	-0.076
$\Delta d_{yz}$	-0.376	-0.372	-0.366	-0.288
$\Delta E$ , eV	-4.130	-3.730	-2.915	-2.489

There are two numbers for the Ni-N overlap population and the Ni electron density changes. The first number refers to the Ni atom toward which the NO bends; the second number refers to the Ni atom from which the NO moves away. As NO bends, the orientation of its  $\sigma$  and  $\pi$  orbitals changes. Among these the  $\pi_y$  orientation changes less and so the  $\pi_y$  electron densities are closer to the linear case, **24a**. However, the interaction for the other  $2\pi$  orbital, with significant components from mixing of  $x$  and  $z$ , **24b**, changes a lot. As a result of this, the electron density in this  $2\pi$  orbital is smaller than in the linear case. Consequently, the NO overlap population becomes larger, that is to say, the N-O stretching frequency should be greater. Therefore this kind of bending is not likely to be the one responsible for the low coverage frequency in the "bent" model.

At bending angle  $90^\circ$  the N-O overlap population is smaller than in the linear case, the oxygen atom comes close to a Ni atom, at a distance of 1.14 Å, and the Ni-O overlap population is a large 0.835. The N-O bond is weakened and the Ni-O overlap population reaches a considerable value. Could this be a geometry for NO dissociation? During the bending the N-Ni overlap populations are quite different for the two nearest Ni atoms. The NO molecule should then move toward the Ni with which it has the larger overlap population, and consequently the  $90^\circ$  bent geometry should have different Ni-O distances. Also,  $\Delta E$  does not favor this bending.

Lehwald et al.<sup>15</sup> gave a picture of NO bending at the twofold bridge site, but toward the threefold hollow site. Our computational results for this kind of bending, **25**, are shown in Table V.



25

At a bending angle of  $30^\circ$ , the results are very close to those at  $0^\circ$ . Bending to  $60^\circ$ , the N-O overlap population decreases by 1%, while the Ni-N overlap population decreases much more, by 14%. This implies a substantial change in Ni-N bonding. The electron density changes less from the original value of 2 in the  $\sigma$  orbitals, as Table V indicates. At  $0^\circ$  the NO  $5\sigma$  orbital interacts with the  $s$ ,  $z^2$ ,  $yz$ , and  $x^2-y^2$  orbitals of the nearest Ni atoms, Ni2 and Ni4 in **25**, with overlaps of 0.147, 0.036, 0.066, and 0.069, respectively.  $5\sigma$  also has considerable overlap with  $p$  orbitals, but the interactions are small because of the relative high energy of

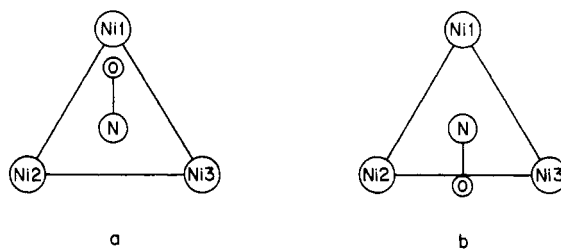
these orbitals. At a bending angle of  $60^\circ$ , the above overlaps decrease to 0.093, 0.017, 0.039, and 0.037, respectively, and consequently the interaction decreases. The interaction between  $5\sigma$  and the second nearest Ni, atoms Ni3 and Ni1 in **25**, is much smaller, compensating for the above decrease. This is why the electron density of  $5\sigma$  changes less at  $60^\circ$ , and it is also the major reason for the decrease of the Ni-N overlap population.

The electron densities in the NO  $\pi$  orbitals change more at a bending angle of  $60^\circ$  than at  $0^\circ$ . The  $2\pi$  electron densities are larger; therefore the N-O overlap population is smaller. The  $2\pi_y$  orbital has a slightly larger electron density in the bent geometry, because it interacts with  $xz$  orbitals of Ni2 and Ni4, with overlap 0.021 at  $60^\circ$ . As NO bends, the  $2\pi_x$  becomes  $2\pi_{x,z}$ , and at a bending angle  $90^\circ$  it becomes  $2\pi_z$ . As NO bends the overlaps of this orbital with the  $xz, xy$  of Ni2 and Ni4 decrease, but the orbital starts to interact with  $s$ ,  $z^2$ ,  $x^2-y^2$ ,  $yz$  orbitals of Ni2 and Ni4. The overlaps with these orbitals increase from 0 to 0.093, 0.036, 0.068, and 0.044, respectively, at  $60^\circ$ . This increase dominates the bonding picture at  $60^\circ$ . This is the reason for  $2\pi_{x,y}$  electron density increase and the N-O overlap population decrease.

In the above analysis we discussed only the interaction with the nearest Ni atoms. In fact other Ni atoms, especially the second nearest Ni (Ni1 and Ni3 in **25**), also participate in the interaction. We picked up only the most important part of the mixing that occurs. For this bending at  $30^\circ$  and  $60^\circ$ , the N-O bonding is weakened ( $\sim 1\%$ ), but not sufficiently to cause any substantial frequency shift. In other words, the NO may bend significantly in the  $yz$  plane without causing substantial N-O bond weakening. However, the Ni-N frequency should decrease substantially when NO bends. When we consider the coverage change at this stage, for example, compare the  $60^\circ$  bending in Table V with  $0^\circ$  and coverage 1, the N-O overlap population changes from 0.958 to 1.012 and the Ni-N overlap population from 0.502 to 0.564. The N-O bond strength change follows the "bending" model, but Ni-N does not. If the change is from bending  $30^\circ$  at coverage  $1/3$  to linear or upright at coverage 1, then the overlap populations change from 0.966 to 1.012 for N-O, from 0.575 to 0.564. This agrees with the experimental observations, according to the "bent" model. However, if the coverage is the only change, i.e., the adsorption system changes from a perpendicular position at coverage  $1/3$  to the same position at coverage 1, we get the same results. From the energetic preferences shown in Table V, the coverage change model is favored over bending.

At the extreme bending angle of  $90^\circ$ , the N-O overlap population increases and becomes higher than that at  $0^\circ$ . Meanwhile the Ni-N bond is substantially weakened. The overlap population between O and Ni1 is 0.521 and their distance is 1.55 Å. The O-Ni2 or O-Ni4 distance is 2.01 Å. The oxygen atom is not exactly at the center of the threefold hollow site. Because the N-O bond is not substantially weakened on going here from an isolated NO molecule, this does not seem to be a likely dissociation geometry.

Bending of NO on a threefold bridge site has been studied for a bending angle of  $\phi = 60^\circ$  in two directions, **26a** and **26b**. The



26

calculational results are shown in Table VI. The N-O overlap populations are larger than for the  $\phi = 0^\circ$  case. The Ni-N overlap population decrease between N and the Ni toward which NO bends (N-Ni1 in **26a** and N-Ni2, N-Ni3 in **26b**) and increase

TABLE VI

	$\phi = 0^\circ$	$\phi = 60^\circ$ (26a)	$\phi = 60^\circ$ (26b)
overlap population			
Ni-N	0.483	0.100 Ni1-N 0.528 Ni2,3-N	0.504 Ni1-N 0.308 Ni2, 3-N
N-O	0.923	1.008	1.065
NO electron densities			
$4\sigma$	1.785	1.722	1.790
$1\pi^a$	1.889	1.874	1.859
$5\sigma$	1.758	1.779	1.786
$2\pi^a$	1.171	1.068	0.993
$\Delta E$ , eV	-4.249	-3.588	-2.118

<sup>a</sup>These are the average values for the two nondegenerate orbitals.

TABLE VII: Extended Hückel Parameters

orbital	$H_{ii}$ , eV	$\zeta_1$	$\zeta_2$	$C_1^a$	$C_2^a$
Ni 4s	-7.8	2.1			
Ni 4p	-3.7	2.1			
Ni 3d	9.9	5.75	2.00	0.568	0.6292
N 2s	-23.6	1.95			
N 2p	-11.5	1.95			
O 2s	-27.0	2.27			
O 2p	-11.6	2.27			

<sup>a</sup>Contraction coefficients used in the double  $\zeta$  expansion.

between N and the atom from which NO bends away (N-Ni2, N-Ni3 in **26a** and N-Ni1 in **26b**). The energy is higher for the bent configuration than it is for the perpendicular one. The computational results show that this kind of bending will not serve to interpret the vibrational frequencies in a bending NO model.

Here we briefly summarize the bending studies. Bending at a threefold site and bending at a twofold site toward the neighboring Ni atom causes an increase in the N-O overlap population. The stretching frequency should then increase, which is inconsistent with the bending model. Bending at the twofold site toward a hollow site causes the N-O overlap population to decrease a little, and bending at the on-top site does the same. In both these cases the Ni-N overlap population decreases, too.

An (NO)<sub>2</sub> dimer model was proposed by Ibach et al.<sup>3</sup> to interpret the spectra of NO on Pt(111). While we have carried out some pilot calculations on alternative geometries for such a dimer, we have not done a systematic study. Our conclusions as to the ability of this dimer to account for the observed spectra are ambiguous, and we defer discussion of them to a later time.

Let us attempt to summarize our findings. At the twofold bridge site, as the coverage increases, the N-O overlap population increases and the Ni-N overlap population decreases. These trends agree with the experimental observations. The possible problem is that the bond strength change seems a little too small to explain

the frequency shift. As the NO changes adsorption site from threefold to twofold bridge or from twofold bridge to the on-top site, the N-O overlap population increases, but N-surface bonding increases as well. As NO changes from bent toward the threefold site in the twofold position to an upright perpendicular position, the N-O overlap population increases a little, as does the Ni-N overlap populations. As NO changes from bent to linear at the on-top site, the N-O overlap population increases substantially, and so does the Ni-N overlap population. Table II provides a brief summary of these computed results.

The bridged adsorption site seems more likely, as the comparison of the observed frequency to that found in molecular complexes indicates. If we do not consider the trend of the Ni-N bonding change as the coverage changes, all of the above configuration changes are consistent with the observed N-O frequency change. If we do accept the possibility that the Ni-N bonding change is in the opposite direction to the N-O bonding change, the consistent explanation is the twofold bridge adsorption with perpendicular or slightly bent (say, 30°) geometry at low coverage and perpendicular geometry at high coverage. This explanation is also consistent with the data for NO on Ni(111) of Madey and of Lehwald, Yates, and Ibach.

*Acknowledgment.* We are grateful to the Office of Naval Research for its support of this work.

## Appendix

In this report all the computations are tight-binding band structure calculations of the extended Hückel type. The  $H_{ii}$ 's for transition metals were obtained from earlier work<sup>22</sup> in this group. The  $H_{ii}$ 's of N and O were determined by charge iteration on NO adsorbed on two sides of a three layer Ni(111) slab model. When NO molecules are adsorbed on both sides of the metal slab, the calculated electron densities on the inner-layer atoms are different from those when NO is adsorbed on one side. However, the electron densities on NO and on the surface metal atoms nearest to NO, which we focus on in this report, are very similar to those in the case of single-face adsorption. All the results listed in this report are from single-face adsorption calculations. Extended Hückel parameters for all atoms used are listed in Table VII.

The geometrical parameters for chemisorption are the Ni-N distance of 1.68 Å and an N-O distance of 1.1 Å from nitric oxide complexes.<sup>30</sup> These distances were used throughout this report. The three layer slab model and a  $k$ -point number equivalent to 10 points for  $1/4$  of the first Brillouin zone were used in all calculations. Each unit cell contains nine metal atoms, except in the part discussing coverage dependence.

**Registry No.** NO, 10102-43-9; Ni, 7440-02-0.

(30) Cox, A. P.; Thomas, L. F.; Sheridan, J. *Nature (London)* **1958**, *181*, 1157.